# AN AUTOMATIC PROCEDURE TO FORECAST TEPHRA FALLOUT

A. Folch (1)(*), C. Cavazzoni (2), A. Costa (1,3) and G. Macedonio (1)

(1) Istituto Nazionale di Geofisica - Sezione "Osservatorio Vesuviano", Napoli, Italy
(2) Consorzio Interuniversitario CINECA, Bologna, Italy
(3) Earth Sciences Department, University of Bristol, U.K.

(*) Corresponding author. Email: afolch@ov.ingv.it

Manuscript submitted to JVGR special volume “Volcanic Flows and Falls” in honour of Prof. M. Sheridan.

**Abstract.** Tephra fallout constitutes a serious threat to communities around active volcanoes. Reliable short-term forecasts represent a valuable aid for scientists and civil authorities to mitigate the effects of fallout on the surrounding areas during an episode of crisis. We present a platform-independent automatic procedure with the aim to daily forecast transport and deposition of volcanic particles. The procedure builds on a series of programs and interfaces that automate the data flow and the execution and subsequent postprocess of fallout models. Firstly, the procedure downloads regional meteorological forecasts for the area and time interval of interest, filters and converts data from its native format, and runs the CALMET diagnostic model to obtain the wind field and other micro-meteorological variables on a finer local-scale 3-D grid defined by the user. Secondly, it assesses the distribution of mass along the eruptive column, commonly by means of the radial averaged buoyant plume equations depending on the prognostic wind field and on the conditions at the vent (granulometry, mass flow rate, etc). All these data serve as input for the fallout models. The initial version of the procedure includes only two Eulerian models, HAZMAP and FALL3D, the latter available as serial and parallel implementations. However, the procedure is designed to incorporate easily other models in a near future with minor modifications on the model source code. The last step is to postprocess the outcomes of models to obtain maps written in standard file formats. These maps contain plots of relevant quantities such as predicted ground load, expected deposit thickness and, for the case of or 3-D models, concentration on air or flight safety concentration thresholds.

## 1. Introduction

Explosive volcanic eruptions can eject into the atmosphere large amounts of blocks, lapilli and ash for relatively long periods of time. These products, globally known as tephra, represent a serious threat for the communities located around active volcanoes. The largest blocks and bombs follow ballistic and non-ballistic trajectories and fall rapidly nearby the volcano. In contrast, ash fragments (from 2 mms to 1 micron in diameter) remain airborne for several hours (or days) and can cover wide areas downwind. The potential effects of volcanic ash on inhabitants and properties include: i) damage to human settlements and buildings including roof collapse by ash loading, corrosion and deterioration of metallic structures, or damage to mechanical and electrical systems, ii) disruption of transportation systems due to loss of visibility, covering of roads and highways, or simply by direct damage to vehicles, iii) disruption to communications due to interference of radio waves or direct damage to communications facilities and electricity failure, iv) temporary shut down of airports or, if the ash trajectory intersects a flight corridor, drifting of aircraft routes to prevent degraded engine performance, loss of visibility, and possible failure of critical navigational and operational instruments that may result from impact with airborne particles, v) chemical and physical changes in water quality of open water-supply systems and increased wear on water-delivery and sewage treatment systems, vi) partial or total destruction of agricultural crops and damage to forestry, vii) destruction of pastures and risk of livestock suffering from fluorosis and other diseases and, to a lesser extent, viii) irritation of eyes and skin and potential respiratory symptoms produced by ash inhalation (for an extensive review on fallout effects see, for instance, the USGS webpage at http://volcanoes.usgs.gov/ash/index.html).

Half a billion people live close to active volcanoes to date (Small and Naumann, 2001). Several tens of cities and urban areas near volcanoes exceed one million inhabitants including Mexico City, Tokyo, Manila, Quito, Seattle and Naples (Chester et al., 2001). Approximately 500 airports lie within 100 km of volcanoes that have erupted during the last hundred years, and tens of thousands of passengers fly over volcanically active regions such as the North Pacific, which has more than 100 active volcanoes and four to five ash-producing eruptions per year (Casadevall, 1993). These data stress the potential socio-economic impacts of volcanoes in general, of tephra fallout in particular, and highlight the relevance of adequate hazard assessment and risk mitigation. Models constitute, together with field studies and monitoring, an essential tool for scientists to achieve this goal. The

utility of models is twofold. On one side, when combined with the study of eruptive products and deposits, they serve to quantify relevant parameters of past events by means of solving an inverse problem. On the other hand, models serve to envisage the characteristics of a future or an on-going event when used in the context of a forward problem assuming expected values for the input parameters. In this sense models are necessary to quantify hazard scenarios and/or to give short-term forecasts during emergency situations.

There are a number of models to predict particle transport and/or the characteristics of the resulting fallout deposits. Different approximations, each presenting advantages and drawbacks, include particle settling and deposition in a wind field (e.g. Carey and Sigurdsson, 1982; Carey and Sparks, 1986; Bursik et al., 1992a; Koyaguchi, 1994; Koyaguchi and Ohno, 2001; Bonadonna and Phillips, 2003), advection-diffusion Eulerian models (e.g. Suzuki, 1983; Armienti et al., 1988; Macedonio et al., 1988; Glaze and Self, 1991; Connor et al., 2001; Bonadonna et al., 2002; Pfeiffer et al., 2005; Folch and Felpeto, 2005; Costa et al., 2006), particle dispersal from umbrella clouds which spread as gravity currents (Bonadonna et al., 1998; Bursik et al., 1992b), and Lagrangian particle tracking (e.g. Heffter and Stunder, 1993; D'Amours, 1998; Searcy et al., 1998; Draxler and Rolph, 2003). A range of complexity can exist within each family of models. The simplest models are obviously less accurate because they rely on hypotheses that simplify the physics in order to derive analytical or semi-analytical solutions for the governing equations. The problem is that oversimplification may result in poor matching between model results and reality. This is specially critical in the case of particle dispersion because the transport phenomenon is mainly ruled by atmospheric properties and, consequently, a poor evaluation of the coupling terms may lead to substantial bias. In contrast, simple models have lower computational requirements and hence are especially suitable to tackle inverse problems and/or to produce immediate gross predictions. Complex models are theoretically more accurate but, in general, require more inputs (not always available), set up times, pre and postprocess data treatment (i.e. possible involuntary manipulation errors), computational requirements and user expertise. All these factors may preclude the efficiency of such models during an episode of pre-eruptive crisis (or, even worst, during the course of an eruption) because they delay the production and delivery of short-term forecasts to the decision-making authorities. An important challenge for the modelling community is to overcome these limitations to advance towards a simultaneously efficient and accurate performance of models.

This paper presents a procedure designed to automate the execution of tephra fallout models and the subsequent interpretation and dissemination of results beyond the scientific community. The goal is to facilitate the execution of models by means of automatic acquisition and manipulation of input data, a subsequent automation of runs and a final shared postprocess analysis. It enables increased performance, eliminates involuntary human manipulation errors, speeds up computing times and anticipates the scientific response during emergencies. Moreover, another non trivial advantage is that the shared postprocess and the production of maps written in portable formats allows for immediate comparison among predictions of different models. Even though the procedure is of general application, it is specially designed as an operational tool to use during volcanic crisis.

## 2. The APOLLO procedure

### 2.1. A general overview

APOLLO (acronym for “Automatic Procedure to mOdeL voLcanic ash dispersiOn”) is a platform-independent automatic procedure designed to create periodic (usually daily) maps with the outcomes of tephra fallout models. The procedure operates as follows. Firstly, a series of programs that perform different tasks generate data eventually needed by models, including a meteorological and terrain database, the definition of the source term, and the granulometric distribution. A meteorological database for a particular area contains short-term predictions, typically up to few days, for meteorological variables (e.g. wind field, temperature, turbulence related variables, etc.) at the nodes of a user-defined 3-D structured grid. The meteorological database(s) is(are) absolutely independent from models and can be created/updated automatically, typically every day as new meteorological prognostics are available for the region(s) of interest. The next stage is to run models which can be launched automatically after the creation/update of a meteorological database or at any user-defined instant. Models and programs read data from control files and databases through a library, named LIBAPOLLO, which contains a set of user-callable routines that act as an interface. Note that, in general, a model is not constrained to use the entire contents of a database. For example, if a model assumes a horizontally uniform wind field, it is sufficient to select a single representative point from each vertical layer of the database. The gathering of values from the database is, consequently, a model dependent step and must be implemented ad hoc for each particular case. The current version of APOLLO contains only the HAZMAP

(Macedonio et al., 2005) and the FALL3D models (Costa et al., 2006). However, the procedure is designed to incorporate other models with minor modifications on the source codes (mainly the inclusion of calls to some routines of the LIBAPOLLO library that gather the input data needed by the model from the APOLLO files and databases). Finally, the last step of the procedure is to postprocess the outcomes from different models in order to produce maps with pre-defined physical quantities. All the models share the same postprocess treatment, so that if two different models output the same quantity (e.g. ground load) their respective maps are directly comparable.

The APOLLO procedure flows by means of scripts that can be launched manually or automatically with a user-defined periodicity (e.g. every day at 8 a.m.). The scripts make calls to models and programs that perform computations or interface tasks (see Figure 1). The user controls the procedure by means of a short ASCII control file that can be modified at any time. It allows, for instance, an eventual incorporation of newly acquired data during an on-going eruption. In contrast, if the control file remains unmodified, the procedure simply runs periodically with the same eruptive parameters but with updated meteorological forecasts. The latter scenario could be characteristic of a pre-eruptive crisis period, during which the eruptive parameters (e.g. mass flow rate, granulometry, etc.) must necessarily be guessed based on the experience from previous events.

### 2.2. The preprocess stage

The preprocess stage creates/updates the meteorological and terrain database(s) as well as the source and the granulometric data files prior to the execution of models. Specifically it involves:

i) To download the files that contain the (mesoscale) meteorological prognostics.

ii) To build a meteorological database for each region of interest. A database contains the topography of the region and relevant prognostic meteorological variables: wind field, air temperature, velocity scales, Monin-Obukhov length, and mixing height. Discrete prognostic values for these variables at different time slices (e.g. every 30 or 60 min) are stored at the nodes of a 3-D grid. This grid of data must be regularly spaced along the horizontal but can have an arbitrary vertical layering. It allows the user to define data grids which are finer in the Atmospheric Boundary Layer (ABL), where gradients of meteorological variables are likely to be important, and coarser at higher vertical levels. In

this version of APOLLO the construction of a meteorological database is based on the program CALMET (Scire et al., 2000).

iii) To create the granulometry and the source files.

This sections describes the role of the different programs devoted to these tasks.

### *2.2.1. The CALMET program*

CALMET (Scire et al., 2000) is an open source meteorological processor developed and maintained by scientists of the US Atmospheric Studies Group (ASG) which includes a diagnostic wind field generator. Assimilating terrain information and an initial guess wind field (in our case, the output of a mesoscale meteorological prognostic model) on a regional and coarse mesh, CALMET computes a zero-divergence wind field and other diagnostic variables on a smaller and finer grid. CALMET uses a terrain following coordinate system, an approach to incorporate the topography normalizing the vertical coordinate by the domain height. For each time slice, the initial guess wind field is first adjusted for: i) kinematic effects of terrain (lifting and acceleration of the air flow over terrain obstacles), ii) thermodynamically generated slope flows and, iii) blocking effects, in order to obtain, after a divergence-minimisation procedure, a step 1 mass-consistent wind field. After that, meteorological observations (if available at the time under consideration), can be added to the step 1 field and an objective analysis procedure eventually gives a second intermediate field. The scheme is designed so that observations are used to correct the step 1 wind field within a user specified radius of influence, whereas it remains unchanged at regions where observations are unavailable. Finally, a new divergence-minimisation procedure is applied iteratively to the step 2 field until the divergence of velocity reaches a lower bound. The final outcome of CALMET consists of values at the grid points for a zero-divergence wind field consistent with the observations (or pseudo-observations) and for other micrometeorological variables like the Monin–Obukhov length, the friction velocity or the atmospheric boundary layer height. These are quantities that may be later required by some fallout models to estimate the eddy diffusivity tensor. It is important to note that the approximation of a zero-divergence wind field assumed by CALMET is fully adequate at heights lower than, or close to, one kilometre (Dutton and Fichtl, 1969), although it is commonly extended up to few kilometres. In consequence, the CALMET output field can only be used confidently for low to medium eruptive columns. In order to automate the execution of CALMET we have developed a set of programs that act as an interface, that is,

that gather data from different sources and create all the input files required by CALMET. These programs are briefly described below.

### *2.2.2. The GEOINP program*

CALMET requires an input file with 2-D geophysical data at ground level. Data in this file include terrain elevation, land use type, surface parameters (surface roughness, albedo, Bowen ratio, soil heat flux and leaf area index) and anthropogenic heat flux. The task of GEOINP (GEOphysical INPut generator) is to write the above parameters at the ground points of the database in a CALMET readable format. To this purpose, the program simply extracts data from a terrain data file and interpolates the geophysical parameters needed by CALMET to the surface points of the database (see Figure 2). The terrain data files are a free format ASCII files that contain a structured grid with data at the nodes. These terrain data grids should ideally cover several hundreds of kilometres around the volcano or volcanic area of interest and, in principle, can have an arbitrary spatial resolution. The value used by default is 1km. Note that, in general, both grids can have different extensions and/or spatial resolutions. The only requirement is that the domain of the database defined by the user, in which both CALMET and fallout models will run, must lay within the bounds of the terrain data grid. This facilitates eventual modifications of terrain data (e.g. a future increase of the data's spatial resolution if a better DEM becomes available, an update of the land use types, etc.) or the progressive addition to the procedure of new regions of the globe. In the latter case one would just need to create a new file with the elevation, the surface parameters and the land use type according to the USGS classification system.

### *2.2.3. The MESOINP program*

As stated previously, CALMET gives the option to use a gridded wind as furnished by a prognostic meteorological model as the initial guess field. Meteorological models solve mass, momentum and energy conservation equations starting from an assumed initial condition (usually based on available sounding observations at the current time) and predict how the variables evolve on the computational grid in order to give forecasts. Governing equations are solved for prognostic variables, but models calculate also diagnostic variables which depend solely upon conditions at the present time. Meteorological models can be divided into synoptic and mesoscale. Synoptic models deal with large-scale meteorological

features (~1000km) and hence operate at global scales. Mesoscale models deal with lower-scale phenomena (form ~10 to ~1000km) and forecast for regional scales. Note that, in any case, a prognostic model runs on a significantly larger horizontal grid spacing (~100km for synoptic and ~10km for mesoscale) and different vertical layering than those defined in the procedure (i.e. than those used by CALMET and the fallout models). CALMET needs therefore to interpolate the guess field from the prognostic model grid. For this reason the use of mesoscale models is preferable, in particular for small to medium-size simulation domains and for low eruptive columns for which the local meteorological features play a major role. The use of global scale models is recommended only for large domains or high eruptive columns.

A revision of the existing mesoscale meteorological models is beyond the scope of this paper. For us, the important point is that the different managing institutions can supply files written in standard formats that contain forecasts at regular time intervals. The choice of a specific mesoscale model may depend upon several factors, but its spatial coverage and the user accessibility to the data are two obvious determinant aspects. Following the directives of the World Meteorological Organization (WMO) the outcomes of mesoscale models are commonly stored using the GRIB (GRIdded Binary) or the netCDF (network Common Data Form) file formats. GRIB is a standard binary format specially conceived to archive and exchange large volumes of gridded data over high-speed telecommunication lines using modern protocols. NetCDF is a set of interfaces for array-oriented data access and a freely-distributed collection of data access libraries that support a machine-independent format for representing scientific data. The purpose of the MESOINP (MESOscale INPut generator) program is to read and decode the necessary GRIB/netCDF files and subsequently merge them into a single ASCII file written in a CALMET readable format. Obviously the number of GRIB/netCDF files required results from the ratio between the database time length (selected by the user) to the mesoscale model output time interval. For instance, to create a database for the next 48 hours using meteorological data provided by a mesoscale model which supplies data at 6 hours intervals, up to 8 GRIB/netCDF files are needed. Although the file formats are standard, the different mesoscale models normally produce distinct output files because they do not consider equal pressure levels and/or they do not output exactly the same physical quantities. For this reason, MESOINP is not a universal decoder and must be particularized for each meteorological model.

### *2.2.4. The CALMETINP program*

The objective of CALMETINP (CALMET INPut file generator) is to write the CALMET control file. This file contains all the information necessary to define a CALMET run (e.g. starting and ending dates, output time interval, grid specification, technical options, etc.). Note that, strictly, the values of the starting and ending dates are the only two records of the CALMET control file that must be updated daily. The modification of other records may seem unnecessary in the context of an automatic procedure. However, a periodic rewriting of the whole CALMET control file opens the possibility to change, at user will, some characteristics of the database (e.g. space resolution and/or extension, time step, time coverage, etc.) each time it is created/updated.

### *2.2.5. The BUILDDBS program*

The role of BUILDDBS (BUILD meteorological DataBaSe) is to create a database file from the outputs of prognostic meteorological models. At this stage, the program admits as input only the CALMET format files (both versions 5.0 and 6.2).

### *2.2.6. The SETSRC program*

Any model of fallout requires a pre-run evaluation of the source term, i.e. it needs an estimation (or, if possible, a measurement) of the mass per unit time and particle class released from the eruptive column. The purpose of SETSRC (SET SouRCe term) is to write a source file with a pre-defined format for each model. Note that, in general, files may differ from one model to another because they are not constrained to use the same spatial or granulometric discretizations (models can run using different vertical layering and/or number of particle classes). The program admits two possibilities. The simplest is just to introduce directly, through the control file, the time-dependency of the mass flow rate and column height. The released mass is, in this case, distributed either among the model nodes that bound the release height or following the empirical Suzuki's parameterization (Suzuki, 1983; Pfeiffer et al., 2005). The second option is more elaborated and involves the solution of the 1-D radial-averaged plume governing equations (Bursik, 2001) that describe the convective region of an eruptive column and allow to solve for the plume centerline position and the mass flux of particles (i.e. to evaluate the mass that falls out of the plume at each point). These equations are intimately coupled with the wind field which, for small to

medium size plumes, may induce a substantial bent-over plume and subsequent variations of plume height and mass release locations. For this reason, the SETSRC program reads the values of the wind field at the database points located above the vent, computes the averaged wind direction, solves the plume governing equations for each time slice of the database and particle class and, finally, projects the results onto the model grid in order to distribute the released mass among the nodes that intersect the trajectory of the plume centerline. Note that the use of a prognostic wind field introduces a time dependence in the source term even if all the eruptive parameters (mass flow rate, class fraction, etc.) are kept constant.

### 2.3. The process stage

The step following the creation/update of the meteorological database and the generation of the source and granulometry files is to run the fallout models. A run is the simulation of a given scenario. The procedure can handle several models simultaneously for a same run involving both serial or parallel executions. Different models can, in principle, have different spatial discretizations but the performance becomes optimal when the spatial discretization of the models (i.e. model mesh points or grid of receptors for Eulerian and Lagrangian models respectively) coincides with the grid of database because, in this case, no interpolation is required from the latter to the former. It is a user's decision to select which model or set of models will run depending on the scope of the simulation and on the characteristics of the eruption. The current version of the procedure incorporates only two Eulerian models, HAZMAP and FALL3D. The original implementation of these models has been slightly modified including the necessary calls to the routines of the LIBAPOLLO library that interface models and input files (i.e. that allow models to recognize the contents and formats of the different input files generated during the preprocess stage).

Eulerian models are based on the solution of the mass conservation equation. Assuming that the main factors controlling atmospheric transport of particles are wind advection, turbulent diffusion and gravity settling, and neglecting particle inertia and effects of particle–particle interaction, the conservation of mass for a given particle settling velocity class yields to:

$$\frac{\partial C_j}{\partial t} + \nabla\left(\mathbf{u}\,\mathrm{C_j}\right) - \frac{\partial}{\partial \mathrm{z}}\left(v_{\mathrm{j}} C_j\right) = \nabla\left(\mathbf{K}\nabla C_j\right) + \mathrm{S_j} \qquad (1)$$

where $t$ denotes time, $C_j(\mathbf{r})$ is the concentration on air of the particle velocity-class $j$, $\mathbf{r}=(x,y,z)$ is the position vector, $v_j(z)$ is the settling velocity of the class $j$ (positive downwards), $\mathbf{u}=(u_x,u_y,u_z)$ is the wind velocity vector, $\mathbf{K}$ is the turbulent diffusion tensor, and $S_j$ the source term. Assuming no interactions among the different velocity classes, because of the linearity of Eq. (1), the total mass is calculated as the sum of the contribution of each settling velocity class. Note that, in the context of the APOLLO procedure, $\mathbf{u}(\mathbf{r},t)$ and $S_j(\mathbf{r},t)$ are evaluated during the preprocess stage.

### *2.3.1.The HAZMAP model*

HAZMAP (Macedonio et al. 2005) is a first-order fallout model. Under the approximations of a constant horizontally uniform wind field and negligible vertical advection and diffusion, Eq. (1) reduces to:

$$\frac{\partial C_j}{\partial t}+u_x\frac{\partial C_j}{\partial x}+u_y\frac{\partial C_j}{\partial y}-\frac{\partial}{\partial z}\left(v_j C_j\right)=K\left(\frac{\partial^2 C_j}{\partial x^2}+\frac{\partial^2 C_j}{\partial y^2}\right)+S_j \qquad (2)$$

where $K$ is the (constant) horizontal turbulent diffusion coefficient. Since the above expression is linear in mass, an instantaneous release of the total mass from the eruption column can be assumed if wind and diffusion parameters do not change significantly with time and just the final deposit is needed. Considering these approximations, Eq. (2) has a semi-analytical solution (see Macedonio et al. (2005) and Pfeiffer et al. (2005) for further details). HAZMAP outputs ground accumulations for each granulometric class. In the context of APOLLO, the quasi-steady approach is assumed to hold for each time slice of the meteorological database, that is, HAZMAP runs once for each time interval of the database considering, in consequence, different wind fields and, eventually, different locations of the source points because the plume centreline may vary at each time step due to different bent-over. Note that, under this approach, the geometry of the final isopachs resulting from the sum of the different time contributions may differ from the classical elliptical shape.

### *2.3.2. The FALL3D model*

During lower magnitude events such as a violent Strombolian eruption, tephra is mostly transported within the ABL, where the simplifying assumptions made to derive Eq. (2) are not longer valid. Wind fields and turbulent tensor components inside the ABL are very complex, temporal variations occur on shorter timescales and topographic effects are, in general, not negligible. Simplified semi-analytical models such as HAZMAP are inadequate for these scenarios in which more complex models like FALL3D (Costa et al., 2006) are needed. FALL3D is a 3-D time-dependent Eulerian model which circumvents most of the simplifications behind the simpler fallout models. The model solves Eq. (1) using a finite differences explicit scheme on a regular terrain-following mesh. It uses the gradient transport theory to evaluate the atmospheric turbulent diffusion within and above the ABL and experimental fits for the particle settling velocities (Ganser, 1993; Dellino et al., 2005). The model can be used to forecast either particle concentration in the atmosphere or particle load on the ground.

An inconvenience of the original serial version of FALL3D is that the computational phase normally lasts few hours. Obviously, computing times are strongly dependent on the characteristics of the grid and number of particle velocity-classes. Just to give an indicative value, a simulation on a desktop Pentium IV PC using a grid with 150×150×10 nodes needs about half minute of CPU time per particle velocity-class and hour of simulated time. This means that a simulation of 48 hours of real time considering 8 granulometric classes requires approximately 3-4 hours of CPU time. These CPU times can be acceptable to model past events but the serial implementation is too inefficient in the context of an automatic procedure. In order to overcome this limitation we have also implemented a parallel version of the code using the Message Passing Interface (MPI) library. The structure of the code combined with the fact that the interaction among particles is a second order effect facilitates the parallelization enormously. Two kinds of parallelization have been considered, one for particle classes and one for space (vertical layers). Firstly, the processors available are distributed among groups or teams. Each team works only on a certain particle class or on a set of particle classes (the number of processors must be, in consequence, a multiple or a divisor of the number of classes). If each particle class has more than one processor assigned (i.e. if the number of processors is a multiple of the number of classes) a second parallelization on the domain is possible. In this case, the tasks within a team are subdivided in vertical layers. Note that it implies a data exchange among processors of the same team but the teams remain isolated among them. The parallelization reaches a limit

when the number of processors in a team equals that of the vertical layers (from ~15 to ~40 depending on the eruptive column height), so that each processor simply solves a 2-D problem for a certain particle class. Excess of parallelization can be prejudicial because the number of interchange operations among processors of a team increases proportionally to the number of members. The scalability analysis shows that best balance is achieved when each CPU works with 3-4 vertical layers. In this case, the performance of the parallel version increases by an order of magnitude with respect to the serial one. It implies CPU times of several minutes for the example mentioned above.

### 2.4. The postprocess stage

The final step of the APOLLO procedure is to postprocess the outcomes of models to produce a set of maps written in portable formats in order to facilitate the dissemination of results. This is done by means of two programs, MODELPOSTP and DBSPOSTP. The former postprocess the results of fallout models whereas the later deals with the visualization of the meteorological database. Both programs output simple 2-D maps in PS (PostScript) and GRD formats. For fallout models that compute ground accumulation (e.g. HAZMAP or FALL3D), MODELPOSTP produces surface maps of deposit load and deposit thickness. For 3-D models that compute also concentration in the air (e.g. FALL3D), MODELPOSTP draws maps of: i) total and class-dependent concentration at different altitudes, ii) z-cumulative concentration per unit area, that is, the integration of concentration along the vertical and, iii) maximum values of concentration along the vertical. The z-cumulative concentration maps give average information about the density of airborne ash and are useful to compare simulations with satellite images. In contrast, the maximum value maps indicate which regions exceed a concentration threshold value that may threaten aircraft operations (Costa et al., 2006). On the other hand, the DBSPOSTP program reads the meteorological database file and generates 2-D maps of the wind field and air temperature at user-selected heights and times. In addition to the generation of 2-D maps, both postprocess programs can output also 2-D and 3-D results in the Visualization Toolkit format in order to facilitate a complementary, more detailed but non-automatic, analysis. The Visualization ToolKit (VTK) is an open-source, freely available software system for 3-D computer graphics, image processing, and visualization. Several widely diffused open-source data postprocess programs are based on the VTK library (e.g. PARAVIEW).

## 3. Application example to the August 1992 Mt. Spurr eruption

Mt. Spurr, an andesitic stratovolcano from the Aleutian arch, Alaska, reawakened with three short but violent vulcanian to sub-Plinan events on June 27, August 18 and September 16, 1992. The events were similar in duration (~4 hours) and intensity, with eruption columns rising up to 14 km a.s.l. (McGimsey, 2001). We have selected the Aug 18 eruption as an application example. It is important to note that our goal is neither to reconstruct in detail the eruptive deposit by means of modelling (i.e. to assess which model input parameters better fit the deposit measurements) nor to reveal the strengths and weaknesses of any particular model. The objective is simply to illustrate the APOLLO procedure using realistic data from a well-documented event. In this sense the results from this section must be understood as a prediction done a few hours (days) prior to the eruption onset, using the prognostic wind field available at that time and the expected values for the eruptive parameters. The Aug 18 event started approximately at 1600h LT (0000h UT Aug 19) and lasted for 3.6 hours with a mean column height of 11.8 km a.s.l. (~9.5 km above the Crater Peak vent). Prevailing winds carried the ash cloud over south-central Alaska including Anchorage, where ash fell as thick as 3 mm, Prince William Sound, and the south-eastern shoreline of the Gulf of Alaska. Ash fallout was concentrated along a narrow belt (~50 km) and a secondary maximum between 130 and 300 km downwind along the deposit axis resulted from fallout aggregates of fine ash of bimodal grain size distribution (Neal et al., 1995; McGimsey et al., 2001). Traces of ash were reported up to 1200 km from the vent. Based on mass per unit area samples, McGimsey et al. (2001) plotted the deposit mass distribution (Figure 3) and estimated a deposit volume of $14\times10^6$ $m^3$ DRE (Dense Rock Equivalent) implying an erupted mass of $36\times10^9$ kg.

Table 1 summarizes the characteristics of the runs as defined in a hypothetical APOLLO control file for Aug 17. The domain of the database, extracted by the GEOINP program from the Alaska terrain file, is a 400×250 km rectangle with a grid resolution of 2 km (Figure 4). Up to 25 vertical layers are defined with a spacing that ranges from 10 m at the ground level to 2 km at the upper one (16 km a.s.l.). The mesoscale meteorological forecasts for Aug 18-19 1992 have been obtained from the NCEP-DOE Reanalysis 2 model (Kanamitsu et al., 2002) as provided by the NOAA/OAR/ESRL PSD, Boulder, Colorado, USA, from the web site at http://www.cdc.noaa.gov/. These data are used by CALMET to compute the 3-D local wind field every 30 minutes for the next 24 hours, that is, for the

defined length of run. We assume a Gaussian granulometric distribution truncated at $\Phi_{min}$=1 and $\Phi_{max}$=7 with the peak at $\Phi_{mean}$=3. The preprocess stage concludes with the creation of the source files by means of the SETSRC program. We consider an eruption duration of 4 hours with an average Mass Flow Rate (MFR) of $2.72\times10^6$ kg/s, a value consistent with the $\sim40\times10^9$ kg of erupted mass estimated by McGimsey et al. (2001). The source term is therefore a step function with a constant value of $2.72\times10^6$ kg/s during the first four hours and zero afterwards. In this example we assume a Suzuki distribution with column height of 13 km above the vent (15.3 km a.s.l.) and Suzuki parameters $A=4$ (maximum mass concentration at 3/4 of the column height) and $\lambda=5$ (high concentration around the maximum). The maximum mass concentration is therefore located at ~9.7 km above the vent (~12 km a.s.l.), a value consistent with the mean column height observed. We have also simulated using a source term given by the plume equations (Bursik, 2001), but differences among both options are not relevant, except at the proximal areas. There are two reasons for this. Firstly, with the granulometry and MFR considered, the plume equations indicate that most particles (90 to 99% depending on the class) fall from the top of the column, predicted at about 11 km a.s.l. Secondly, the eruptive column is large enough to avoid being substantially bent-over by the surrounding wind field (the average wind intensity of ~8 m/s induces only ~10º of plume inclination).

The next stage is to run the fallout models. Computing times on a laptop Pentium IV PC are, for this particular example, ~1 minute for HAZMAP and ~2 hours for the FALL3D serial version (~15 minutes for the parallel version of the code using 12 CPU's of a cluster). Figure 5 shows the deposit load predicted by HAZMAP and FALL3D. Note that the HAZMAP model is quasi-steady and, as a consequence, the mass released during each time slice of the database (in this particular example 30 minutes) settles instantaneously on a constant wind. For this reason the HAZMAP deposit remains unmodified after 4 hours, when the source term vanishes (i.e. when the eruption ends). In contrast, the FALL3D model is transient and hence the ash cloud is affected by wind variations (winds change while particles are still airborne) and the fallout culminates several hours after the end of the eruption. This is reflected in Figure 6, which shows the temporal evolution of both deposits. It follows that the latter model predicts a deposit morphology and main axis orientation which, qualitatively, seem to agree better with the observations (Figure 3). Note also how FALL3D reflects the topographic relief on the isopachs. Deviations from the classical elliptical shapes result from a combined effect of the topography itself and the presence of higher vertical wind components at valleys (down-slope flows). Neither HAZMAP or

FALL3D are able to reproduce the observed secondary maximum because aggregation of particles is not contemplated in these particular models. In addition to predicting the characteristics of the deposit, 3-D transient models like FALL3D can also compute the temporal evolution of concentration in the air. Figure 7 shows the z-cumulative concentration (vertical integration along the 16 km of height range) at different times. Results compare quite well with satellite images of the Advanced Very High Resolution Radiometer (AVHRR) band 4 minus band 5 brightness temperature difference. For volcanic clouds, the magnitude of the negative brightness temperature difference depends, among other factors, upon the optical thickness of the cloud (Prata, 1989) and hence these satellite images can be directly compared with the z-cumulative concentration. Figure 8 plots, for different time slices, the concentration at two vertical levels and the maximum value of concentration along the vertical predicted by the FALL3D model. The latter is a quantity related to the aerial navigation safety. Unfortunately, at present there are no agreed values of concentration which constitute a hazard to jet aircraft engines. Assuming, just for illustrative purposes, that concentration values higher than $0.5\text{-}5\times10^{-3}$ gr/m$^3$ jeopardize or impede aircraft operations, the shaded regions in Figure 8 must be understood as a conservative estimation for any height of flight.

## 4. Summary and conclusions

We have developed a platform-independent procedure to automate the periodic forecast of tephra transport and deposition. Although its general applicability, the tool is especially conceived to obtain reliable short-term forecasts during pre-eruptive crisis episodes. Whenever new meteorological prognostic data for the next few days become available (typically every 12 or 24 hours) the procedure can launch a series of programs and models without user intervention. It includes: i) extraction of terrain data from a terrain data file, ii) download and decoding of files with mesoscale meteorological forecasts and merging into a single file, iii) execution of the prognostic meteorological processor CALMET to get a 3-D regional wind field and other micrometeorological variables of interest, iv) construction of a meteorological and terrain database, v) construction of the files with the granulometric distribution and the source terms and, vi) execution and postprocess of the fallout models selected by the user among those available (at the moment only HAZMAP and FALL3D). A single control file allows for eventual modifications of parameters from run to run (e.g. location and/or extension of the computational domain, variation of the eruptive parameters, etc.). For each model under consideration the procedure can output GRD and PS format files that contain 2-D maps of interesting quantities such as predicted ground load, expected deposit thickness or visual and flight safety concentration thresholds. These are low to medium graphical quality files conceived for eventual mailing or downloading via a website. In addition, the procedure can output also VTK format files for a non-automatic, more sophisticated 2-D and 3-D postprocess.

Some advantages of the APOLLO procedure are:

i) Modularity. Each program of the procedure performs a specific task and runs independently from the rest. It gives large flexibility and facilitates future modifications or addition of new functionalities.

ii) Flexibility. There is an absolute flexibility concerning the quantity of meteorological databases and number of runs. For instance, different databases for different regions can coexist and be updated with different periodicity (e.g. every 6 hours, daily, etc.). It allows, for instance, to automate forecasts for several volcanoes or volcanic areas simultaneously. On the other hand, there is no limit on the number of runs for a specific location (several runs can use the same meteorological database). Thus, for example, one could consider different runs starting at the same time instant (e.g. to model an event supposed to start after 24 hours but considering different scenarios characterized by different mass flow rates or

column heights), different runs starting at different time instants (e.g. to model a single scenario supposed to start after 24, 48 or 72 hours), or both.

iii) Automatization. The scripts that control the flow of the procedure can be launched periodically without user intervention. It speeds up the production of results and precludes from user manipulation errors.

iv) Data sharing. All the models run using the same input data and can share also the same postprocess. It ensures that outcomes (maps) from different models in the same run are directly comparable.

v) Model/data independency. Models and data interface through a library (the LibApollo). It guarantees that future changes in the formats of files will not affect models and vice-versa. New models can be added to the procedure with minor changes in the source codes.

Computing times are logically dependent on the selected model and size of the computational domain. Simplest first-order models (e.g. HAZMAP) run 'instantaneously', even for large domains and/or high grid resolutions. However, predictions may in this case deviate notably from observations, especially for low eruptive columns (in which an appreciable part of the transport phenomenon occurs within the ABL) and/or for short lived eruptions. More sophisticated 3-D transient models (e.g. FALL3D) require larger computational times and resources. For example, the 18 hour Mt Spurr simulation on a 200×125×25 node mesh considering 7 granulometric classes takes about 2 hours on a Pentium IV laptop PC (15 minutes using 12 CPU's of a cluster). The total time required by the APOLLO procedure (including pre and postprocess) for this particular case is ~2.5 hours (~45 minutes on the cluster). It implies a time lag between the reception of meteorological data and the production of maps which may be reasonable even in our context. However, larger domains and/or simulation times would require the use of a cluster for the procedure to be efficient.

**Acknowledgements**. This work has been supported by the INGV project "Sviluppo Nuove Tecnologie per la Protezione e Difesa del Territorio dai Rischi Naturali" and the HPC-EUROPE Transnational Access Program. We wish to thank C. Bonadonna and L. Glaze for their constructive reviews of the manuscript and R. Gori and G. Erbacci from CINECA (Bologna, Italy) for their support on the implementation of the postprocess code.

## References


Armienti, P., Macedonio, G., Pareschi, M., 1988. A numerical model for the simulation of tephra transport and deposition: applications to May 18, 1980, Mt. St. Helens eruption. J. Geophys. Res. 93 (B6), 6463–6476.

Bursik, M., 2001. Effect of wind on the rise height of volcanic plumes. Geophys. Res. Lett. 18, 3621–3624.

Bursik, M.I., Sparks, R.S.J., Gilbert, J., Carey, S.N., 1992a. Sedimentation of tephra by volcanic plumes. I. Theory and its comparison with a study of the Fogo A Plinian deposit Sao Miguel (Azores). Bull. Volcanol. 54, 329– 344.

Bursik, M.I., Carey, S.N., Sparks R.S.J., 1992b. A gravity current model for the May 18, 1980 Mount-St-Helens plume. Geophys. Res. Lett. 19, 1663-1666.

Bonadonna, C., Ernst, G., Sparks, R.S.J., 1998. Thickness variations and volume estimates of tephra fall deposits: the importance of particle Reynolds number. J. Volcanol. Geotherm. Res. 81, 173– 187.

Bonadonna, C., Macedonio, G., Sparks, R.S.J., 2002. Numerical modelling of tephra fallout associated with dome collapses and Vulcanian explosions: application to hazard assessment on Montserrat. In: T. Druitt, B. Kokelaar (Eds.), The Eruption of Soufriére Hills Volcano, Montserrat, from 1995 to 1999. Geol. Soc. Lond., pp. 517–537.

Bonadonna, C., Phillips, J.C., 2003. Sedimentation from strong volcanic plumes. J. Geophys. Res., 108(B7), 2340, doi:10.1029/2002JB002034.

Carey, S., Sigurdsson, H., 1982. Influence of particle aggregation on deposition of distal tephra from the May 18, 1980, eruption of Mount St-Helens volcano. J. Geophys. Res. 87 (B8), 7061–7072.

Carey, S., Sparks, R.S.J., 1986. Quantitative models of the fallout and dispersal of tephra from volcanic eruption columns. Bull. Volcanol. 48, 109– 125.

Casadevall, T. J., 1993. Volcanic Ash and Airports - Discussion and Recommendations from the Workshop on Impacts of Volcanic Ash on Airport Facilities. U.S. Geological Survey Open-File Report, 93-518, 52 pp.

Chester, D.L., Degg, M., Duncan, A.M., Guest, J.E., 2001. The increasing exposure of cities to the effects of volcanic eruptions: a global survey. Environ. Haz., 2, 89-103.

Connor, C., Hill, B., Winfrey, B., Franklin, M., La Femina, P., 2001. Estimation of volcanic hazards from tephra fallout. Nat. Hazards Rev. 2, 33–42.

Costa, A., Macedonio, G., Folch, A., 2006. A three-dimensional Eulerian model for transport and deposition of volcanic ashes. Earth Planet. Sci. Lett., 241 (3-4), 634-647.

D'Amours, R., 1998. Modeling the ETEX plume dispersion with the Canadian emergency response model. Atmos. Environ. 32 (24), 4335–4341.

Dellino, P., Mele, D., Bonasia, R., Braia, G., La Volpe, L., Sulpizio, R., 2005. The analysis of the influence of pumice shape on its terminal velocity. Geophyis. Res. Lett. 32, 21306-21309.

Draxler, R.R., Rolph, G.D., 2003. HYSPLIT (HYbrid Single-Particle Lagrangian Integrated Trajectory) Model access via NOAA ARL READY Website (http://www.arl.noaa.gov/ready/hysplit4.html). NOAA Air Resources Laboratory, Silver Spring, MD.

Dutton, J., Fichtl, G., 1969. Approximate equations of motion for gases and liquids. J. Atmos. Sci. 26, 241– 254.

Folch, A., Felpeto, A., 2005. A coupled model for the dispersal of tephra during sustained explosive eruptions. J. Volcanol. Geotherm. Res. 145 (3–4), 337–349.

Ganser, G., 1993. A rational approach to drag prediction spherical and non-spherical particles. Powder Technol. 77, 143–152.

Glaze, L., Self, S., 1991. Ashfall dispersal for the 16 September 1986 eruption of Lascar, Chile, calculated by a turbulent diffusion model. Geophys. Res. Lett. 18, 1237–1240.

Heffter, J., Stunder, B., 1993. Volcanic Ash Forecast Transport and Dispersion (Vaftad) model. Weather Forecast 8, 533–541.

Kanamitsu, M. ,Ebisuzaki, W., Woollen, J., Yang, S-K., Hnilo, J.J., Fiorino, M., Potter, G.L., 2002. NCEP-DEO AMIP-II Reanalysis (R-2), Bul. of the Atmos. Met. Soc., 1631-1643.

Koyaguchi, T., 1994. Grain-size variation of the tephra derived from umbrella clouds. Bull. Volcanol. 56, 1–9.

Koyaguchi, T., Ohno, M., 2001. Reconstruction of the eruption column dynamics on the basis of grain size of tephra fall deposits. 1. Metods. J. Geophys. Res. 106 (B4), 6499–6512.

Macedonio, G., Pareschi, M., Santacroce, R., 1988. A numerical simulation of the Plinian fall phase of the 79 AD eruption of Vesuvius. J. Geophys. Res. 93 (B12), 14817–14827.

Macedonio G., Costa A., Longo A., 2005. A computer model for volcanic ash fallout and assessment of subsequent hazard. Computer and Geosciences, 31 (7), 837-845.

McGimsey, R.G., Neal, C.A., Riley, C.M., 2001. Areal Distribution, Thickness, Mass, Volume, and Grain Size of Tephra-Fall Deposits from the 1992 Eruptions of Crater Peak Vent, Mt. Spurr Volcano, Alaska. Open-File Report 01-370, U.S.G.S., Alaska Volcano Observatory, Anchorage.

Neal, C.A., McGimsey, R.G., Gardner, C.A., Harbin, M.L., Nye, C.J., Keith, T.E.C., 1995. Tephra-fall deposits from the 1992 eruptions of Crater Peak, Mount Spurr Volcano, Alaska; a preliminary report on distribution, stratigraphy, and composition, in T.E.C. Keith (ed), The 1992 eruptions of Crater Peak Vent, Mount Spurr volcano, Alaska, pp. 65-79, U. S. Geological Survey, Reston, VA.

Pfeiffer, T., Costa, A., Macedonio, G., 2005. A model for the numerical simulation of tephra fall deposits. J. Volcanol. Geotherm. Res., 140, 273-294.

Prata, A.J., 1989. Infrared radiative transfer calculations for volcanic ash clouds. Geophys. Res. Lett., 16, 1293-1296.

Scire, J., Robe, F., Yamartino, R., 2000. A User's Guide for the CALMET Meteorological Model. Tech. Rep. Version 5, Earth Tech, Inc., 196 Baker Avenue, Concord, MA 01742.

Searcy, C., Dean, K., Stringer, W., 1998. Puff: a high-resolution volcanic ash tracking model. J. Volcanol. Geotherm. Res. 80, 1–16.

Small, C., Naumann, T., 2001. The global distribution of human population and recent volcanism. Environ. Haz. 3, 93-109.

Suzuki, T., 1983. A theoretical model for dispersion of tephra. In: D. Shimozuru, I. Yokoyama (Eds.), Arc Volcanism: Physics and Tectonics, Terra Scientific Publishing Company (TERRAPUB), Tokyo.

## List of figures

**Figure 1**. APOLLO flowchart. Light grey boxes indicate inputs of the procedure (terrain data, meteorological forecasts and other parameters defined in the run and meteorological database control files). Dark grey boxes indicate the programs and models included in the procedure and described in the text.

**Figure 2**. The procedure incorporates terrain data files for different regions of interest with a spatial resolution of 1km. The figure shows, as an example, the extension of the file for South Italy, which covers a 800×800 km area. Axes show UTM coordinates in km (UTM zone 33). The user-defined domain, which holds the database and serves also to run CALMET and the fallout models, has a lower extension and can have a different spatial resolution. The program GEOINP interpolates data from the former to the latter and writes a CALMET readable format file with the characteristics of the terrain.

**Figure 3**. Mass distribution of the Aug 18, 1992 Mt. Spurr fallout deposit. Values indicate the deposit load in $gr/m^2$. Points mark the locations of samples and observations. Axes show UTM coordinates in m (UTM zone 6). After McGimsey et al. (2001).

**Figure 4**. Extension of the domain used in the Mt. Spurr runs. Axes show UTM coordinates in km (UTM zone 5).

**Figure 5**. Deposit load predictions for HAZMAP (top) and FALL3D (bottom) models. Axes are in UTM coordinates (zone 6) in km with the origin at (500,6650). Grid lines every 50 km. Contour values of 0.1, 1, 2, 5, and 10 $kg/m^2$. Results for HAZMAP are shown at Aug 19 0400h UT (4 hours after the eruption onset) whereas results for FALL3D are at Aug 19 1800 UT. See the text for explanation.

**Figure 6**. Variation of the deposit load with time for HAZMAP (black contours) and FALL3D (red contours). Contour values are in $kg/m^2$. Results at Aug 19 0100h, 0200h, 0400h, and 1800h UT. HAZMAP is quasi-steady and, as a consequence, all the mass falls during the first 4 hours. In contrast, FALL3D is transient and hence most particles still remain airborne for several hours after the eruption end.

**Figure 7**. z-cumulative concentration (vertical integration) predicted by FALL3D at Aug 19 0100h, 0300h, and 0600h UT respectively. Contours of 100 gr/$m^2$ plotted. AVHRR satellite images at approximately the same times are also shown at the top right corner for comparison.

**Figure 8**. FALL3D predictions for concentration at two vertical levels of 5000 and 10000 m (red lines) and maximum value of concentration along the vertical (black lines) at Aug 19 0100h, 0600h, 1200h, and 1800h UT respectively. A single contour of $10^{-6}$ kg/$m^3$ ($10^{-3}$ gr/$m^3$) is shown for illustrative purposes. Assuming this value to be a threshold for flight operations, the shaded area marks a conservative bound for safety.

| Parameter | Value |
|---|---|
| Computational domain | 400×250×16 km (200×125×25 points) |
| Starting date | Aug 18 1600 LT (Aug 19 0000 UT) |
| Eruption duration [(1)] | 4h |
| Length of run | 18h |
| Vent location [(1)] | 61º18'N 152º15'W |
| Wind field | From NCEP-DOE Reanalysis 2 meteorological model |
| Database time step | 30 min |
| Averaged mass flow rate [(1)] | $2.72\times10^6$ kg/s |
| Averaged plume height [(1)] | 9.5 km above the vent (11.8 km a.s.l.) |
| Granulometry [(2)] | Gaussian with $\Phi_{min}=1$, $\Phi_{max}=7$, $\Phi_{mean}=3$ and $\sigma_\Phi=1.5$ |
| Number of classes | 20 (HAZMAP) and 7 (FALL3D) |
| Particle density [(2)] | 2000 kg/m$^3$ for $\Phi<3$ and 2500 kg/m$^3$ for $\Phi\geq3$ |
| Terminal velocity model | Ganser (1993) |
| Turbulent diffusion [(2)] | $K$=2500 m$^2$/s (HAZMAP) |
| | Variable. Given by the gradient transport theory (FALL3D) |

**Table 1**. List of values considered for the Aug 19 1992 Mt. Spurr application case. [(1)]Quantity observed or derived from measurements (McGimsey, 2001). [(2)]Quantity guessed.

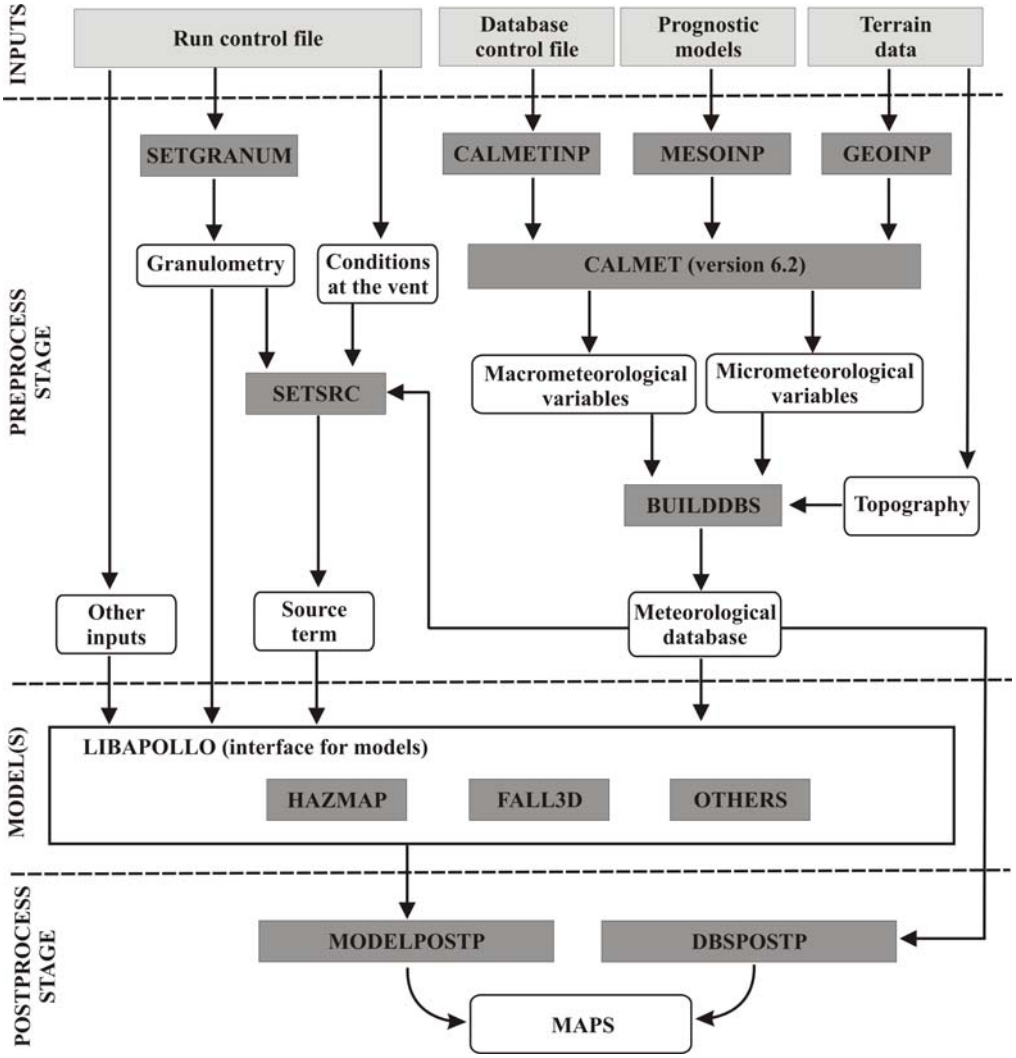
INPUTS
Run control file
Database control file
Prognostic models
Terrain data
SETGRANUM
CALMETINP
MESOINP
GEOINP
PREPROCESS STAGE
Granulometry
Conditions at the vent
CALMET (version 6.2)
SETSRC
Macrometeorological variables
Micrometeorological variables
BUILDDBS
Topography
Other inputs
Source term
Meteorological database
MODEL(S)
LIBAPOLLO (interface for models)
HAZMAP
FALL3D
OTHERS
POSTPROCESS STAGE
MODELPOSTP
DBSPOSTP
MAPS

**Figure 1**

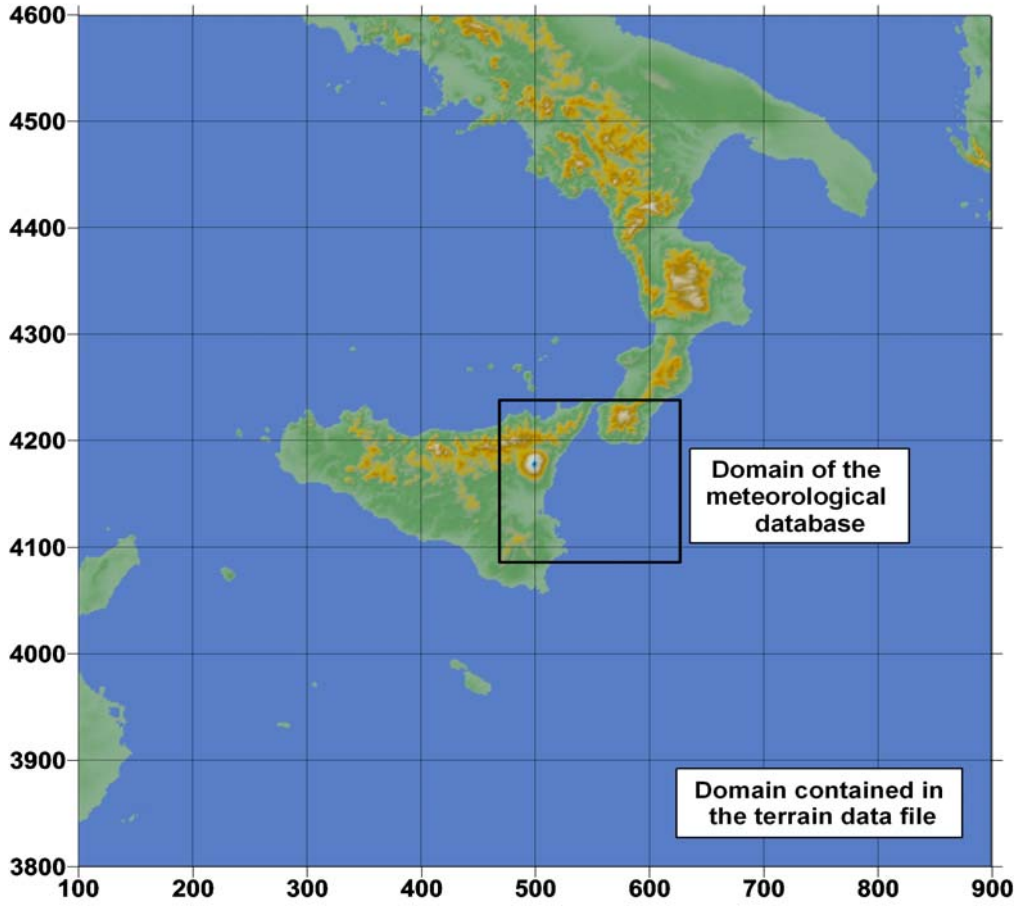
4600
4500
4400
4300
4200
4100
4000
3900
3800
100
200
300
400
500
600
700
800
900
Domain of the meteorological database
Domain contained in the terrain data file

**Figure 2**

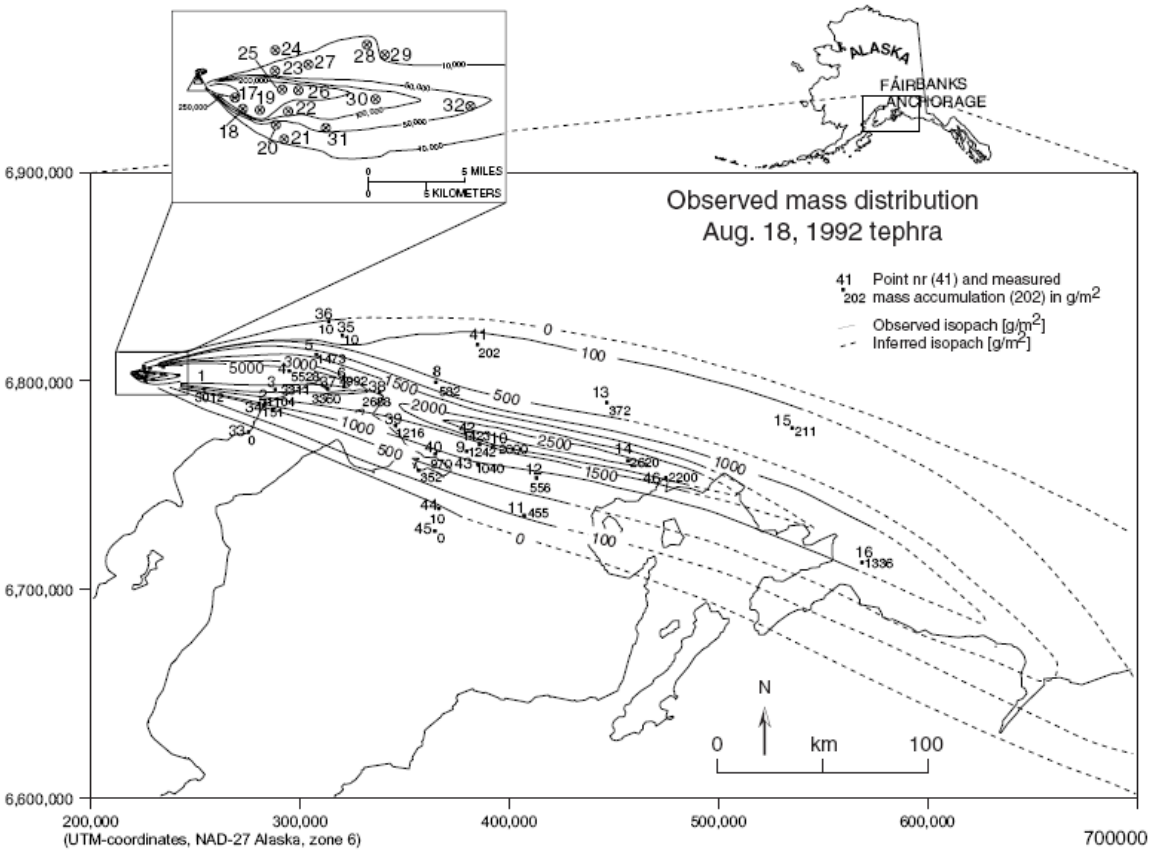
ALASKA
FAIRBANKS
ANCHORAGE
Observed mass distribution
Aug. 18, 1992 tephra
41 Point nr (41) and measured
202 mass accumulation (202) in g/m2
Observed isopach [g/m2]
Inferred isopach [g/m2]
5 MILES
5 KILOMETERS
N
0 km 100
6,900,000
6,800,000
6,700,000
6,600,000
200,000
300,000
400,000
500,000
600,000
700000
(UTM-coordinates, NAD-27 Alaska, zone 6)

**Figure 3**

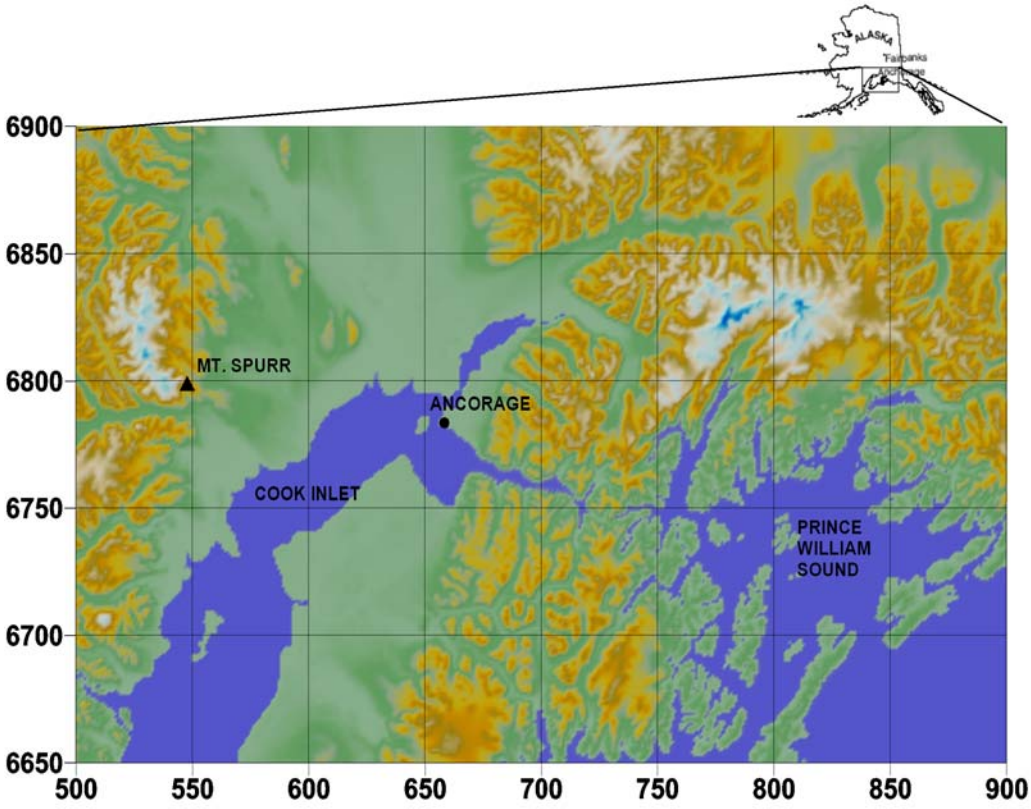
ALASKA
Fairbanks
Anchorage
6900
6850
6800
6750
6700
6650
500
550
600
650
700
750
800
850
900
MT. SPURR
ANCORAGE
COOK INLET
PRINCE
WILLIAM
SOUND

**Figure 4**

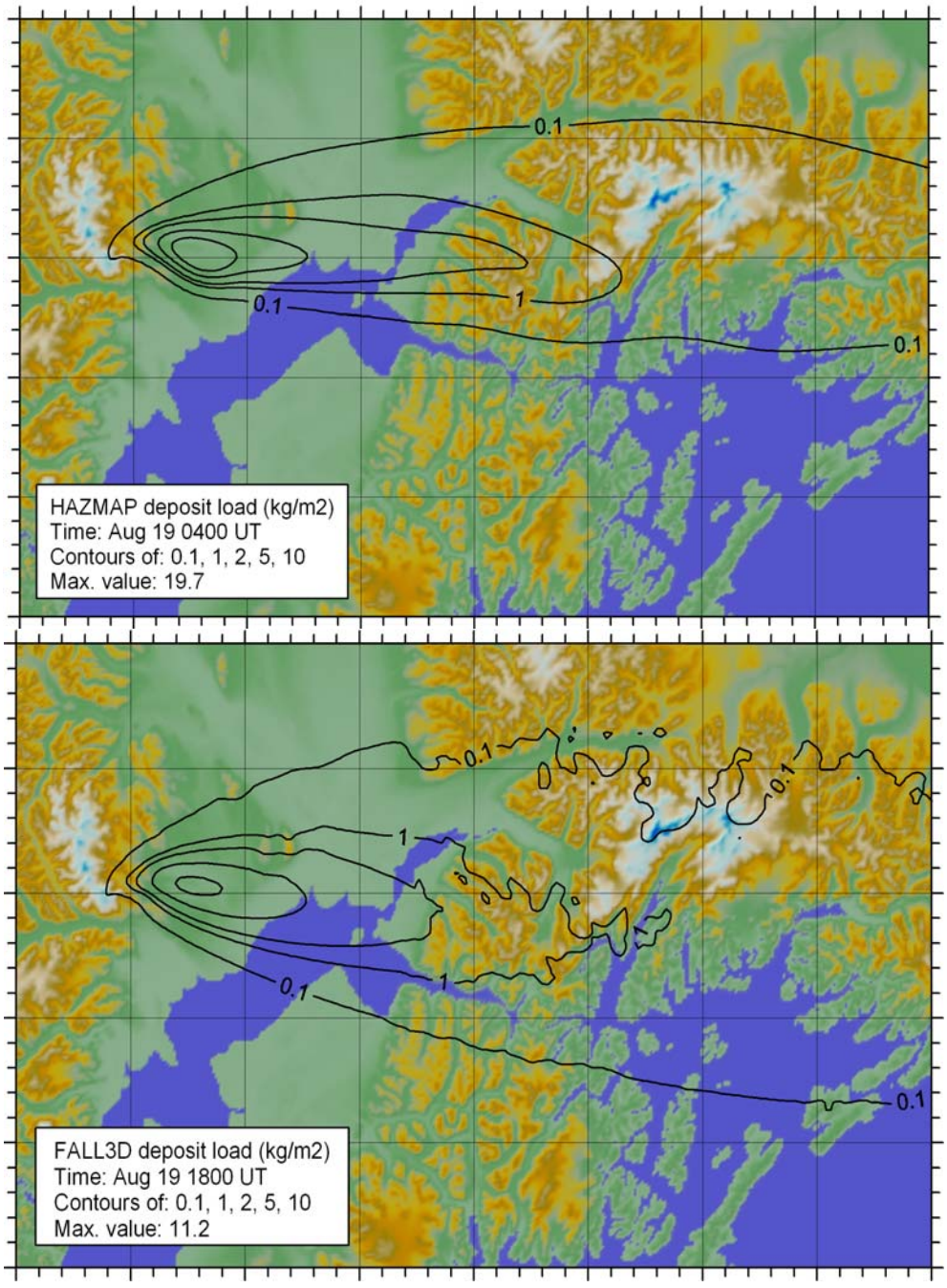
0.1
1
0.1
0.1
HAZMAP deposit load (kg/m2)
Time: Aug 19 0400 UT
Contours of: 0.1, 1, 2, 5, 10
Max. value: 19.7
0.1
0.1
1
1
0.1
0.1
FALL3D deposit load (kg/m2)
Time: Aug 19 1800 UT
Contours of: 0.1, 1, 2, 5, 10
Max. value: 11.2

**Figure 5**

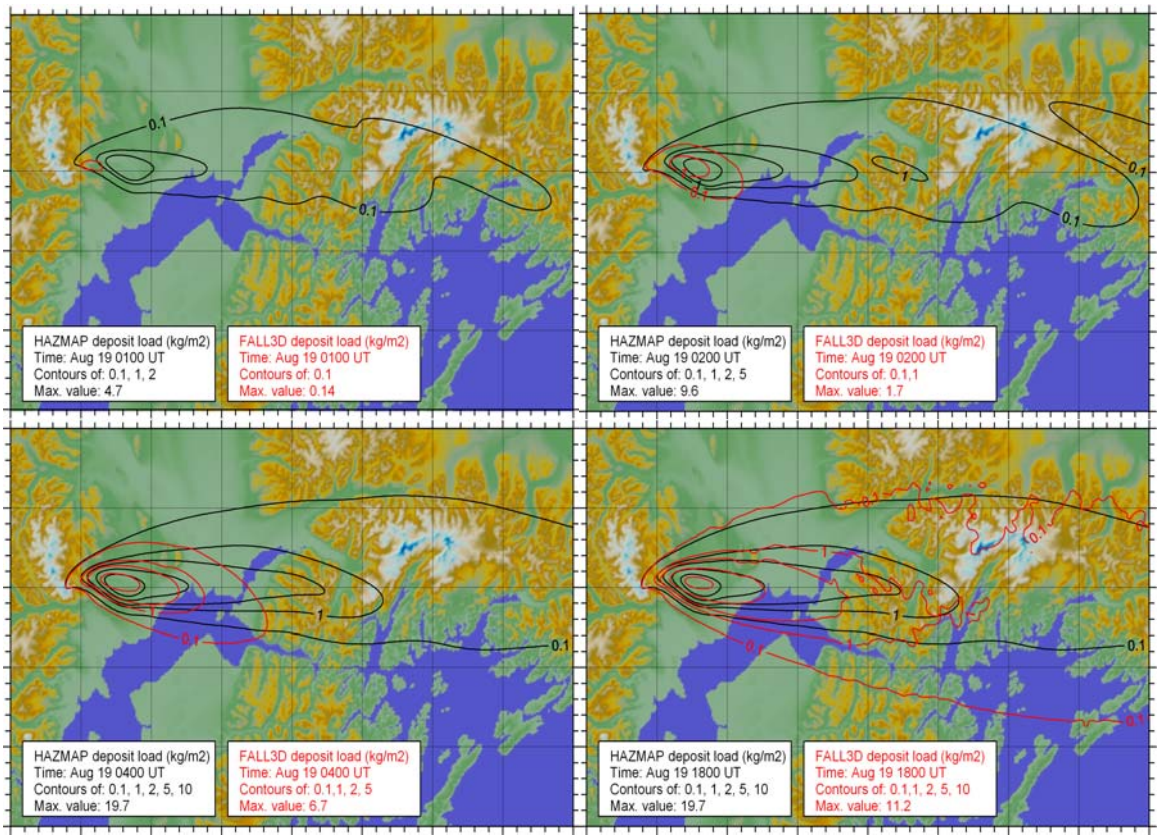
HAZMAP deposit load (kg/m2)
Time: Aug 19 0100 UT
Contours of: 0.1, 1, 2
Max. value: 4.7
FALL3D deposit load (kg/m2)
Time: Aug 19 0100 UT
Contours of: 0.1
Max. value: 0.14
HAZMAP deposit load (kg/m2)
Time: Aug 19 0200 UT
Contours of: 0.1, 1, 2, 5
Max. value: 9.6
FALL3D deposit load (kg/m2)
Time: Aug 19 0200 UT
Contours of: 0.1,1
Max. value: 1.7
HAZMAP deposit load (kg/m2)
Time: Aug 19 0400 UT
Contours of: 0.1, 1, 2, 5, 10
Max. value: 19.7
FALL3D deposit load (kg/m2)
Time: Aug 19 0400 UT
Contours of: 0.1,1, 2, 5
Max. value: 6.7
HAZMAP deposit load (kg/m2)
Time: Aug 19 1800 UT
Contours of: 0.1, 1, 2, 5, 10
Max. value: 19.7
FALL3D deposit load (kg/m2)
Time: Aug 19 1800 UT
Contours of: 0.1,1, 2, 5, 10
Max. value: 11.2

Figure 6

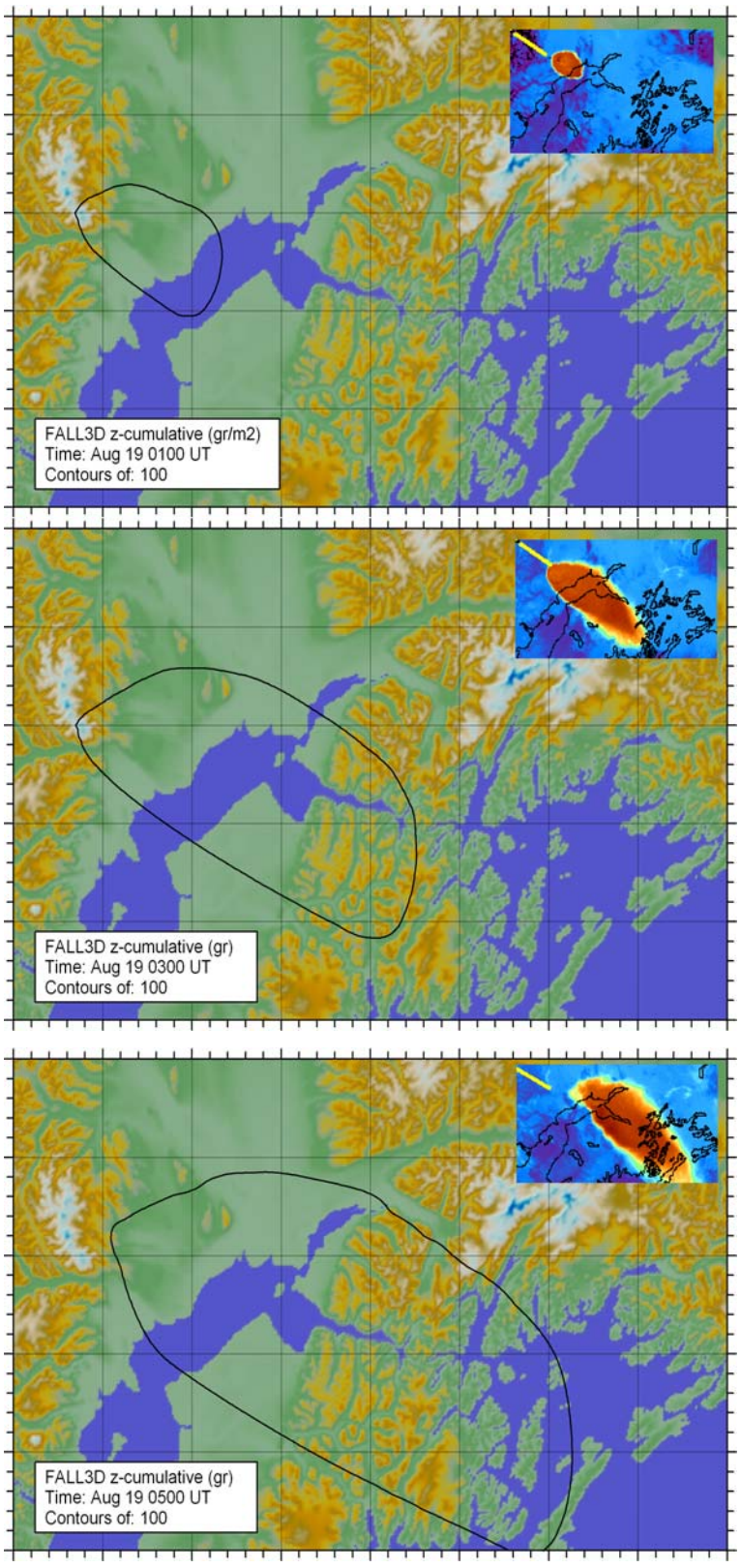
FALL3D z-cumulative (gr/m2)
Time: Aug 19 0100 UT
Contours of: 100
FALL3D z-cumulative (gr)
Time: Aug 19 0300 UT
Contours of: 100
FALL3D z-cumulative (gr)
Time: Aug 19 0500 UT
Contours of: 100

**Figure 7**

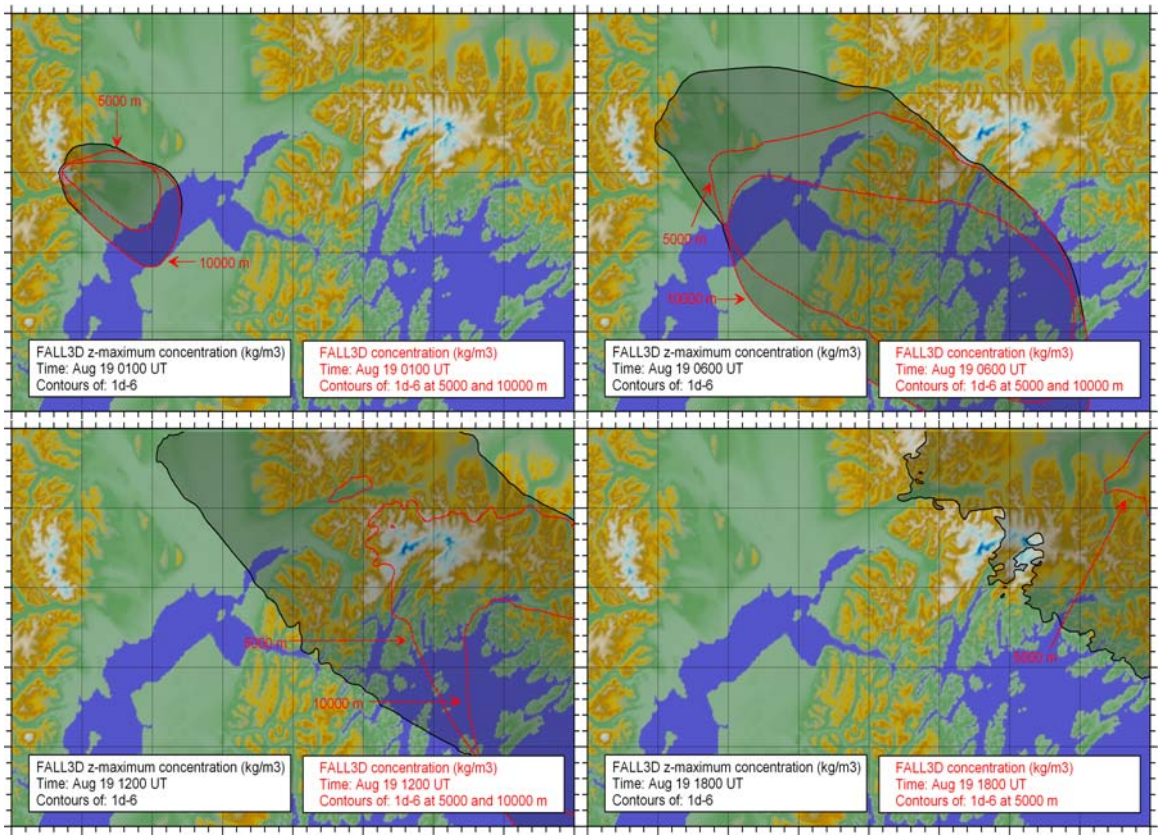
5000 m
10000 m
FALL3D z-maximum concentration (kg/m3)
Time: Aug 19 0100 UT
Contours of: 1d-6
FALL3D concentration (kg/m3)
Time: Aug 19 0100 UT
Contours of: 1d-6 at 5000 and 10000 m
5000 m
10000 m
FALL3D z-maximum concentration (kg/m3)
Time: Aug 19 0600 UT
Contours of: 1d-6
FALL3D concentration (kg/m3)
Time: Aug 19 0600 UT
Contours of: 1d-6 at 5000 and 10000 m
5000 m
10000 m
FALL3D z-maximum concentration (kg/m3)
Time: Aug 19 1200 UT
Contours of: 1d-6
FALL3D concentration (kg/m3)
Time: Aug 19 1200 UT
Contours of: 1d-6 at 5000 and 10000 m
5000 m
FALL3D z-maximum concentration (kg/m3)
Time: Aug 19 1800 UT
Contours of: 1d-6
FALL3D concentration (kg/m3)
Time: Aug 19 1800 UT
Contours of: 1d-6 at 5000 m

Figure 8